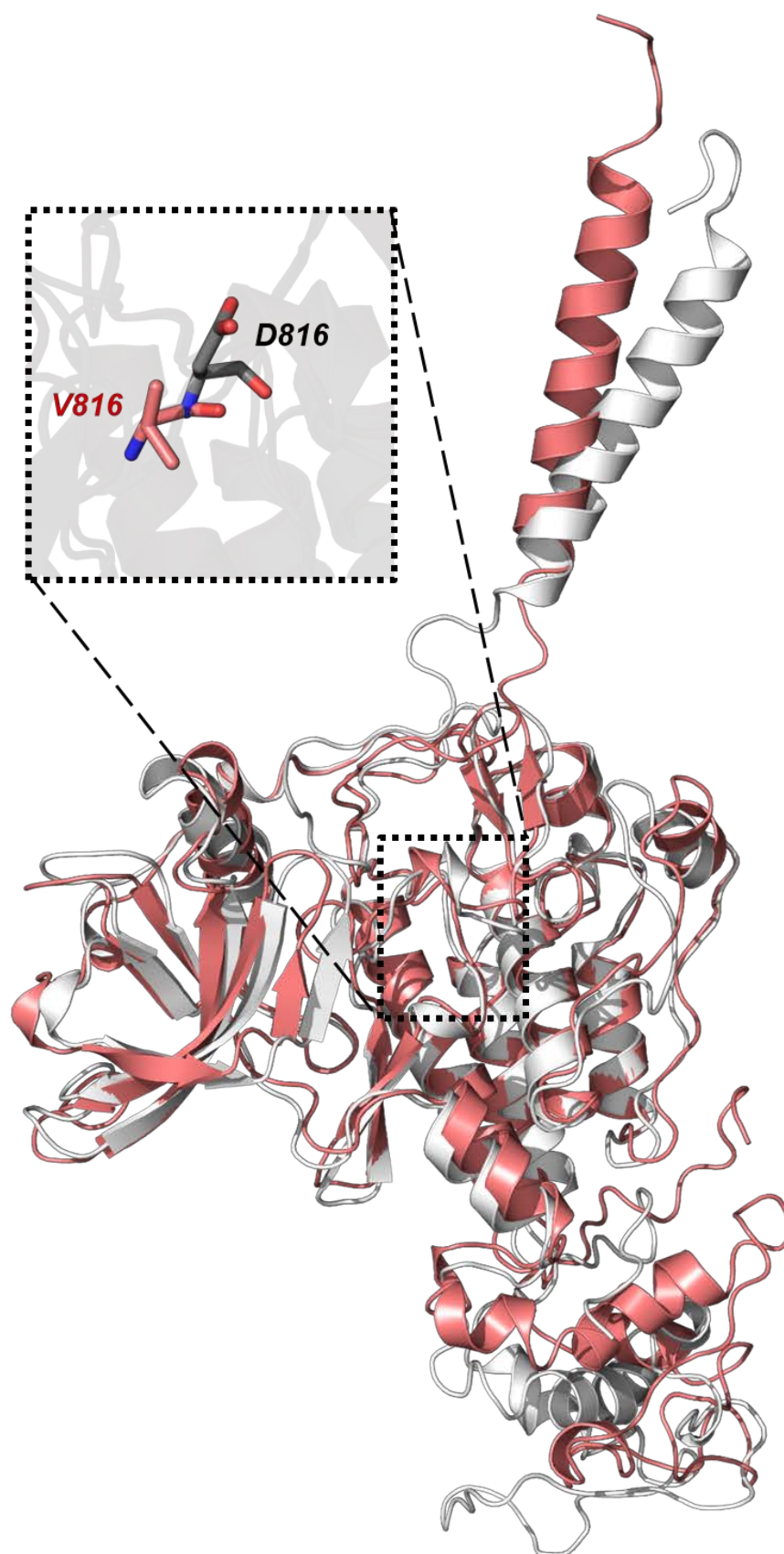# Supplementary Material

Receptor Tyrosine Kinase KIT: Mutation-Induced Conformational Shift Promotes Alternative Allosteric Pockets

Julie Ledoux, Marina Botnari and Luba Tchertanov[*]

Figures S1-S6

Tables S1-S2

Figure S1. Homology modelling of KIT^D816V from the KIT^WT full-length cytoplasmic domain model completed by the transmembrane helix (sequence I516-R946). Superimposition of KIT^WT (in grey) taken at t=2 μs of MD simulation, and KIT^D816V (in pink) taken at t = 0 μs. RMSDs calculated on C-alpha after fitting on tyrosine kinase domain is of 6.5 Å.
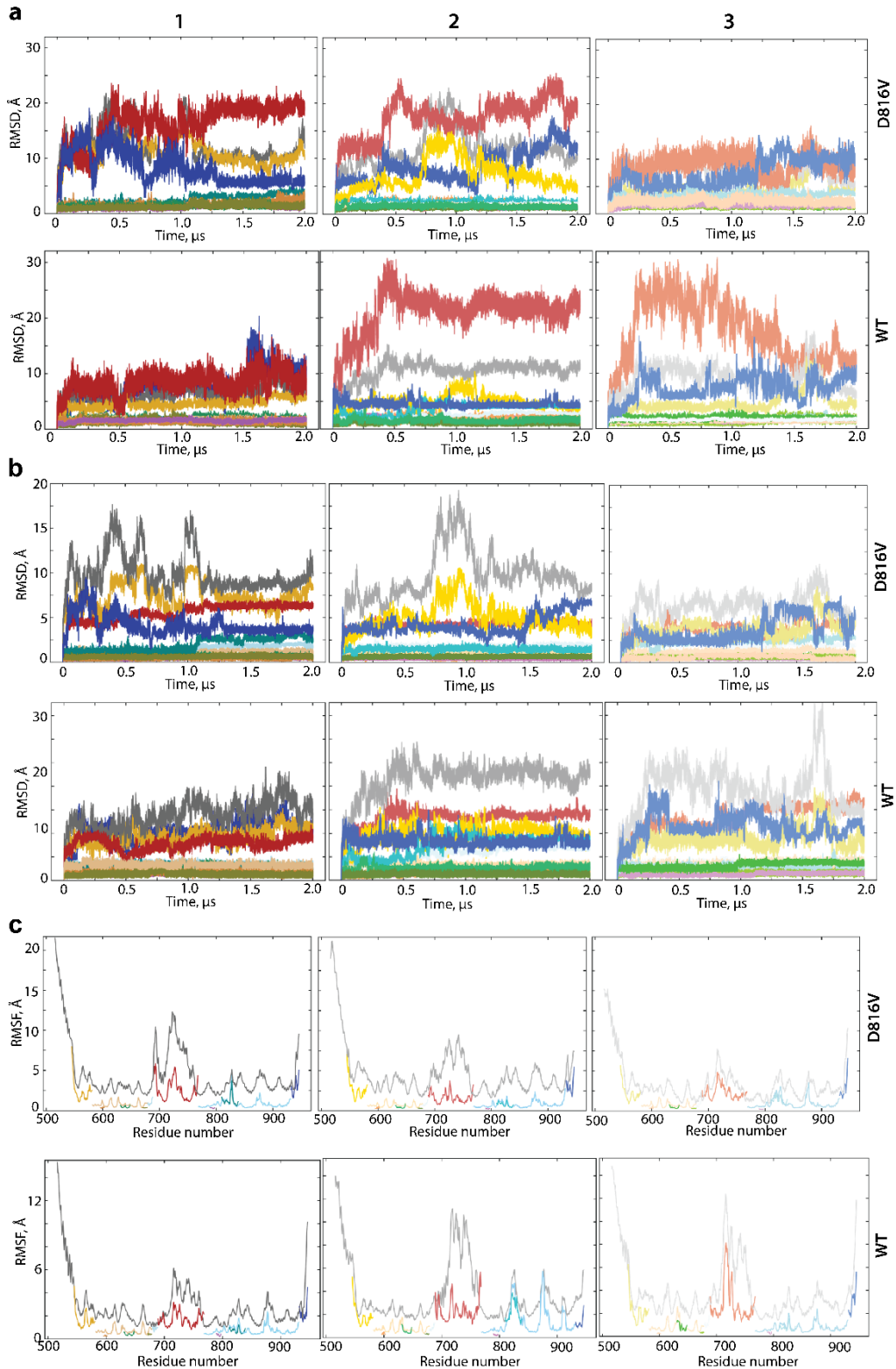
Figure S2. Molecular Dynamics (MD) simulations of the full-length cytoplasmic domain of KIT^{D816V} and KIT^{WT}. (**a**) RMSDs computed on the Cα atoms after fitting on initial conformation (at t = 0 ns) (1-3 replicas, each of 2 μs) of kinase domain and each domain/region of KIT^{D816V} (**a**) and KIT^{WT} (**b**). (**c**) RMSFs computed on the Cα atoms for MD conformations after the least-square fitting on the kinase domain initial conformation of KIT^{D816V} (top panel) and KIT^{WT}. (**a-c**) KIT is in grey, N-lobe in beige, C-lobe in blue, JMR in yellow, P-loop in orange, αC-helix in green, hinge in olive, KID in red, C-loop in magenta, A-loop in teal, C-tail in dark blue for the 1-3 trajectories (replicas) of MD simulations. MD replicas 1-3 are distinguished by colour tonality, dark, lighter, and light.

3
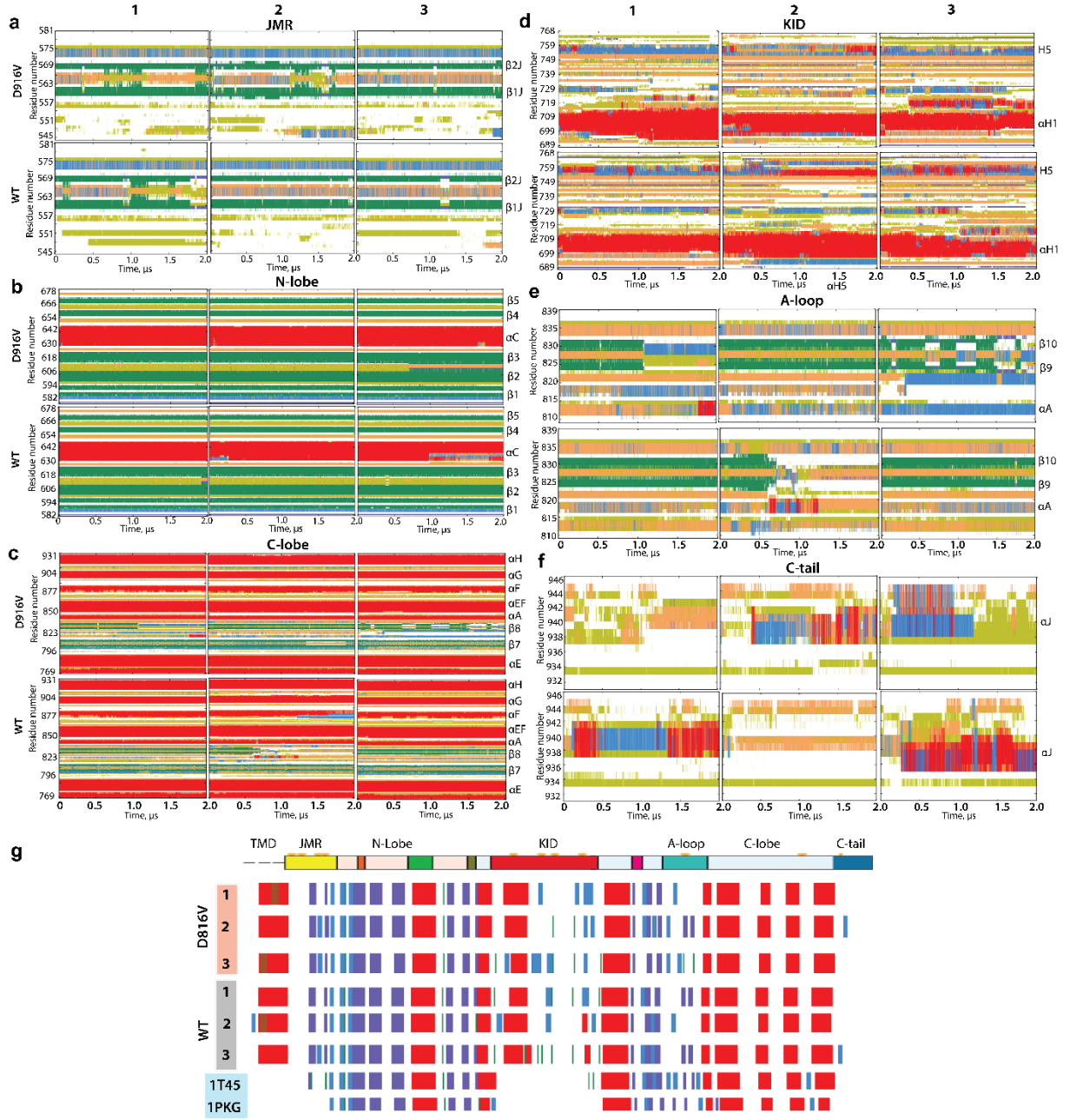
Figure S3. Folding of KIT[D816V] (top panels) and KIT[WT] (bottom panels). (**a-f**) The time-related evolution of the secondary structures of the entire, full-length KIT and per domain/region, as assigned by DSSP: α-helices in red, 3₁₀-helices in blue, parallel β strands in green, antiparallel β strands in dark blue, turns in orange, and bends in dark yellow. The three cMD replicas (1–3) were analysed individuially. (**g**) The secondary structures—αH- (red), 3₁₀-helices (light blue), and β-strands (dark blue)—assigned for a mean conformation of every MD trajectory (1–3) of KIT[D816V], KIT[WT] and the crystallographic structures 1T45 (inactive KIT) and 1PKG (active KIT). (**D**) The secondary structures—αH- (red) and β-strands (dark blue)—assigned on the mean conformation of the concateneted trajectories.

4
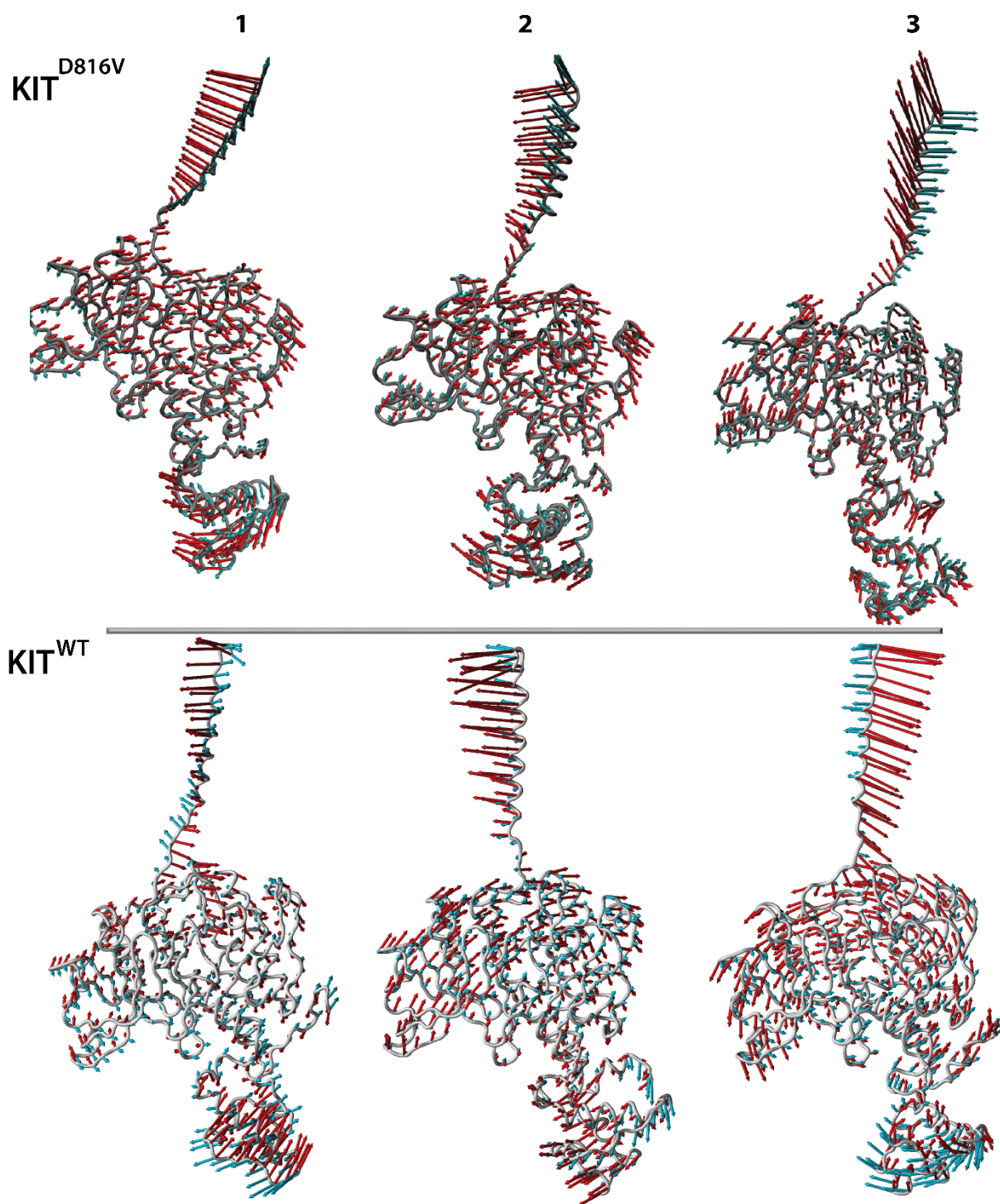
Figure S4. PCA of the MD conformations of KIT. Atomic components in PCA modes 1–2 are drawn as red (1st mode) and cyan (2nd mode) arrows, projected on the cartoon of KIT^{D816V} (top) and KIT^{WT} (bottom). PCA was performed on each individual trajectory of KIT^{D816V} and KIT^{WT}. A cut-off distance of 4 Å was used.
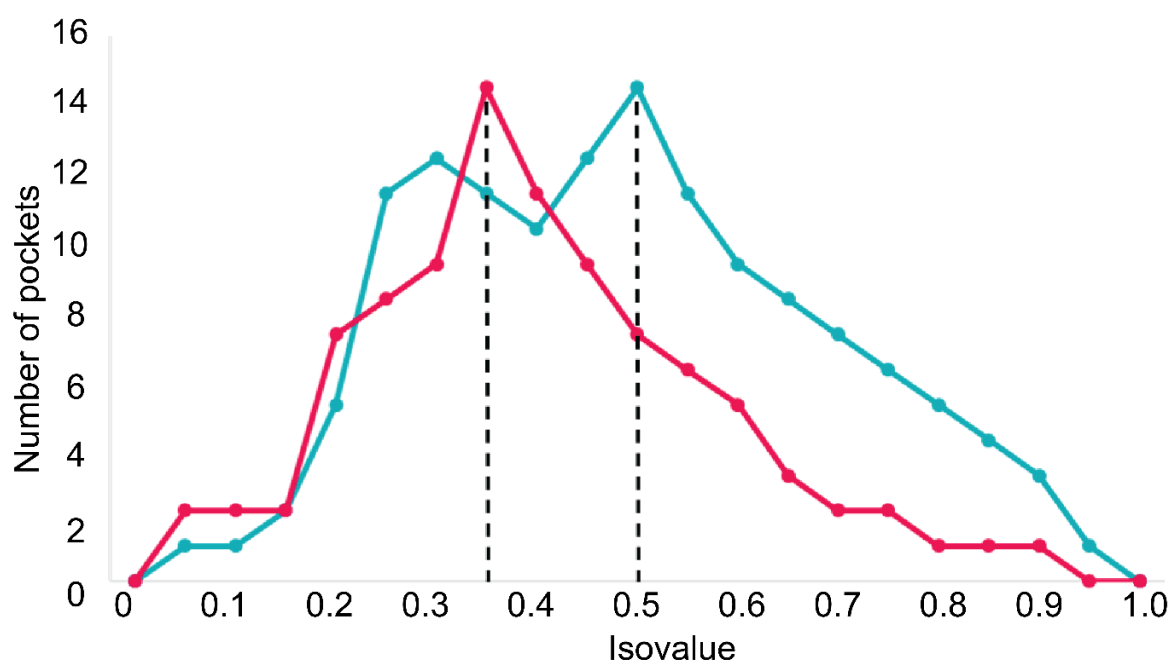
Figure S5. Search of the optimal criteria for pockets hunting. This step is carried out using the isovalue from 0 to 1.0 with a step of 0.5 for both proteins. KIT[D816V] and KIT[WT] are in red and cyan respectively.
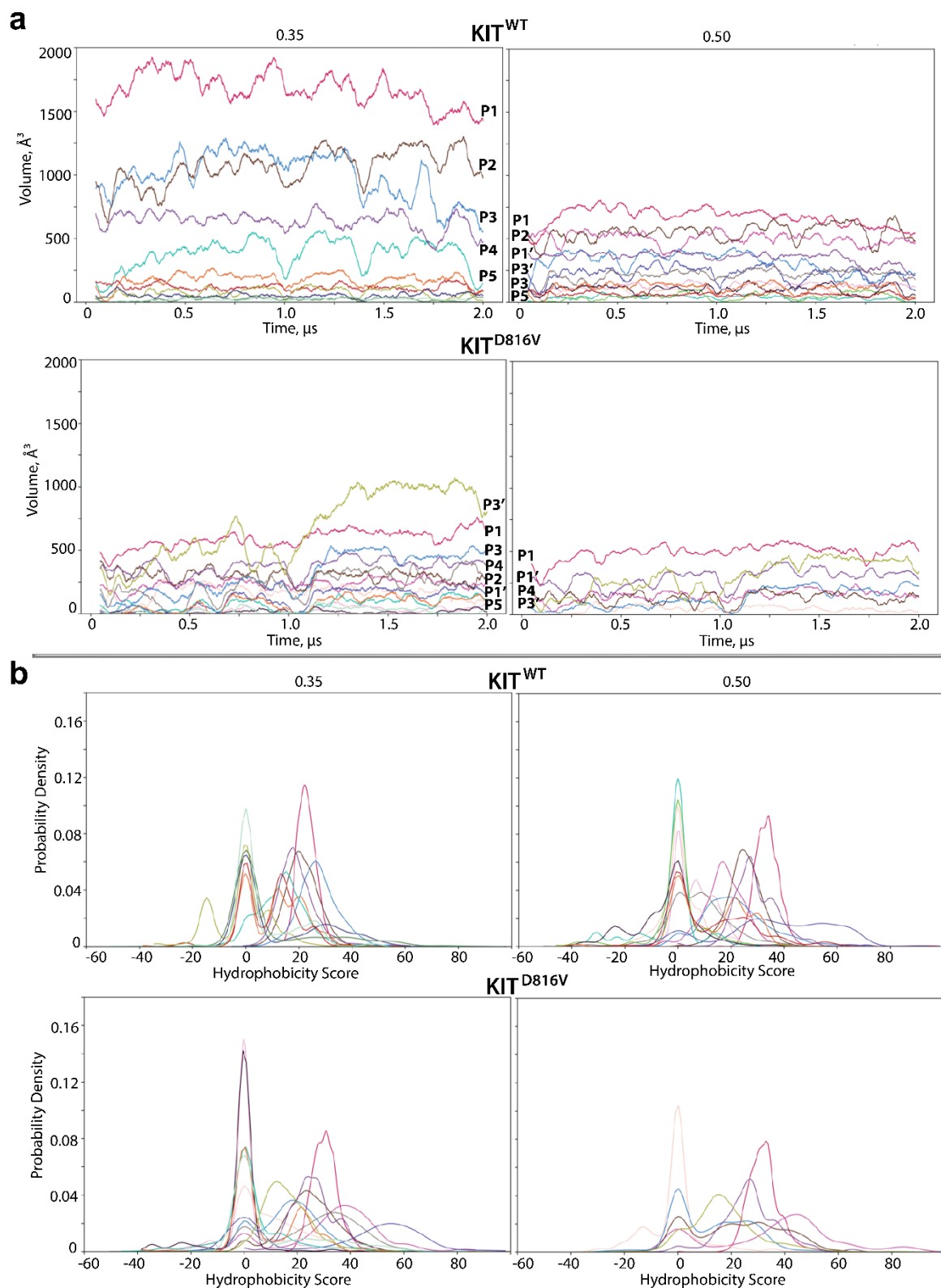
Figure S6. The RTK KIT POCKETOME characterisation. (**a**) The pockets evolution over the simulation time in each KIT protein. (**b**) Probability of the pockets hydrophobicity defined as in (Monera *et al.*, 1995). The pockets are distinguished by colour as defined in Figure 8.

Table S1. Folding of the intrinsically disordered regions in KIT^{WT} and KIT^{D816V}

	KIT^{WT} mean folding (%)			KIT^{D816V} mean folding (%)		
	Helix	**Strand**	**Total**	**Helix**	**Strand**	**Total**
JMR	13 ± 4	14 ± 0	27 ± 4	10 ± 4	16 ± 2	29 ± 5
KID	30 ± 8	3 ± 2	33 ± 5	32 ± 5	2 ± 2	33 ± 7
A-loop	**3 ± 3**	**13 ± 9**	**17 ± 5**	**13 ± 5**	**9 ± 8**	**22 ± 9**
C-tail	13 ± 9	0	13 ± 9	15 ± 11	0	15 ± 11

Table S2. Pockets characterisation in KIT^{WT} and KIT^{D816V}. The numbering of the pocket (P1-P6) is presented as in Figure 8, characterised by the volume size (V_{max}, Å^3), measured in the frame (Frame) and formed by the number of residues (N res). Pockets were characterised by the Fpocket algorithm using isovalue of 0.35.

	KIT^{WT}			KIT^{D816V}			
Pocket	**V_{max}, Å^3**	**Frame**	**N res**	**Pocket**	**V_{max}, Å^3**	**Frame**	**N res**
P1	2674.9	521	72	**P1/ P1'/ P1''**	993.7/574.2/218.0	1907	24/10/11
P2	1757.9	1649	38	**P2/P2'**	704.2/652.57	1850	44/9
P3	1818.9	668	43	**P3/P3'/P3''**	216.0/830.7/379.7	1199	4/25/8
P4	873.9	1499	20	**P4**	688.5	1760	23
P5	1076.9	1511	26	**P5**	382.8	1785	5
P6	421.4	724	11	**P6**	295.7	744	5